



A Journal of the Gesellschaft Deutscher Chemiker

Angewandte Chemie

GDCh

International Edition

www.angewandte.org

Accepted Article

Title: Can a poison be a gift? the role of alkali metal in the α -MnO₂ catalyzed ammonia selective catalytic reaction

Authors: Zhifei Hao, Zhurui Shen, Yi Li, Haitao Wang, Lirong Zheng, Ruihua Wang, Guoquan Liu, and Sihui Zhan

This manuscript has been accepted after peer review and appears as an Accepted Article online prior to editing, proofing, and formal publication of the final Version of Record (VoR). This work is currently citable by using the Digital Object Identifier (DOI) given below. The VoR will be published online in Early View as soon as possible and may be different to this Accepted Article as a result of editing. Readers should obtain the VoR from the journal website shown below when it is published to ensure accuracy of information. The authors are responsible for the content of this Accepted Article.

To be cited as: *Angew. Chem. Int. Ed.* 10.1002/anie.201901771
Angew. Chem. 10.1002/ange.201901771

Link to VoR: <http://dx.doi.org/10.1002/anie.201901771>
<http://dx.doi.org/10.1002/ange.201901771>

Can a poison be a gift? the role of alkali metal in the α -MnO₂ catalyzed ammonia selective catalytic reaction

Zhifei Hao,^{[+][a]} Zhurui Shen,^{[+][b]} Yi Li,^[c] Haitao Wang,^[a] Lirong Zheng,^[d] Ruihua Wang,^[a] Guoquan Liu,^[a] and Sihui Zhan^{*[a]}

Dedicated to the 100th anniversary of Nankai University

Abstract: *The unexpected phenomenon and mechanism of the alkali metal involved NH₃-SCR catalyst were reported here. It is found that the incorporation of K⁺ (4.22 wt %) in the tunnels of α -MnO₂ greatly improved its activity in low temperature (50-200 °C, 100 % conversion of NO_x vs. 50.6 % conversion over pristine α -MnO₂ at 150 °C). Thereafter, experimental and theoretical evidences demonstrated the atomic role of incorporated K⁺ in α -MnO₂. Results showed that K⁺ in the tunnels could form a stable coordination with eight nearby O_{sp3} atoms. The columbic interaction between the trapped K⁺ and O atoms can rearrange the charge population of nearby Mn and O atoms, thus making the topmost five-coordinated unsaturated Mn cations (Mn_{5c}, the Lewis acid sites) more positive. Therefore, the more positively charged Mn_{5c} can better chemically adsorb and activate the NH₃ molecules compared with its pristine counterpart, which is crucial for subsequent reactions.*

For decades, the alkali metal species are highly involved in the catalytic chemistry.^[1] Besides as the active sites in the organic homogeneous catalysis,^[2] the alkali metal species can also efficiently promote the performance of heterogeneous catalysis via multiple ways. The recent examples include: 1) The alkali metal cations can stabilize the metastable active sites,^[1a] e.g. mononuclear Au-O(OH)_x species were well stabilized by K⁺ or Na⁺.^[1b] 2) In-situ formed alkali metal compound coatings (e.g. the Li, K, Cs molten salt) on active sites can elevate the catalytic activity by the co-adsorption effect.^[1c, 1d] 3) They can control the chemical compositions of active sites and the corresponding catalytic performance,^[1e] e.g. the active sites can be changed into Cu-Co alloy or Co/Co₂C by changing the content of Na⁺.^[1f] 4)

The alkali metal species can also directly react with the out-most surface of active sites and then change their physiochemical properties.^[1g] These advances have shed light on further promotion of heterogeneous catalysis using alkali metal species. However, restrictions are arising from the limited knowledge of how the alkali metal species play their roles at atomic-level. This is important for developing novel catalysts and thus necessary to be investigated.

Lewis acid sites can dominate many important homogeneous or heterogeneous catalytic reactions.^[3] For example, asymmetric organic synthesis,^[3a] catalytic polymerization toward macromolecules and heterogeneous industrial catalytic reactions.^[3b, 3c] It is known that the chemical nature of Lewis acid sites are positively charged centers,^[4] no-matter they are nonmetal (e.g. Boron),^[4a] metal (e.g. Ni²⁺, Ce³⁺) or atomic clusters (e.g. Ni, Au),^[4b, 4d] which can attract the electrons and then initiate the reactions. Therefore, it is crucial to understand and control the electronic structure of Lewis acid sites, which would bring new strategy for better activating the Lewis acid sites.

Herein, we have focused on NH₃ selective catalytic reactions (NH₃-SCR) among various Lewis acid sites correlated reactions, due to its importance for cleaning NO_x from power plants and mobile diesel vehicles.^[5] It is known that the alkali metal species can promote catalytic performance in many conditions. However, they are typical poisons for most NH₃-SCR catalysts e.g. V₂O₅-WO₃/TiO₂ ^[5a, 5b] and α -MnO₂.^[5c] Generally, the reaction temperature should be above 300 °C to decompose the alkali metal species, which is energy consuming. High conversion of NO_x at lower temperature is one of the key scientific issues for NH₃-SCR. Therefore, the anti-alkali metal ability of the catalyst is usually necessary to achieve a lower reaction temperature. Unexpectedly, in this study, we have found that the incorporation of K⁺ (4.22 wt %) in the tunnels of α -MnO₂ could greatly improve its activity at 150 °C in NH₃-SCR (100 % conversion of NO_x vs. 50.60 % conversion over pristine α -MnO₂). Although several literatures have inserted the K⁺ in the tunnels of α -MnO₂, hardly any of them captured similar phenomenon in the current work.^[6] Thereafter, experimental and theoretical evidences have demonstrated the atomic role of incorporated K⁺ in α -MnO₂, which brought a K-O eight coordination and the charge rearrangement of the nearby Mn and O atoms, resulted in more positively charged and better activated Mn_{5c} Lewis acid sites.

Kinds of α -MnO₂ nanorods were fabricated here as the model catalysts for NH₃-SCR reaction, including: K⁺ in its tunnels (K- α -MnO₂), K⁺ on its surface (K/ α -MnO₂) and pristine α -MnO₂ nanorod. The quantity of K⁺ was determined by the

[a] Z.F. Hao, R.H. Wang, G.Q. Liu, Prof. H.T. Wang, Prof. S.H. Zhan
MOE Key Laboratory of Pollution Processes and Environmental Criteria
Tianjin Key Laboratory of Environmental Remediation and Pollution Control
College of Environmental Science and Engineering, Nankai University
Tianjin 300350 (P. R. China)
E-mail: sihuizhan@nankai.edu.cn

[b] Prof. Z.R. Shen
School of Materials Science and Engineering, Nankai University
Tianjin 300350 (P. R. China)

[c] Prof. Y. Li
Tianjin Key Laboratory of Molecular Optoelectronic Sciences
Department of Chemistry, School of Science, Tianjin University
Collaborative Innovation Center of Chemical Science and Engineering
Tianjin, 300072 (P. R. China)

[d] Dr. L. Zheng
Beijing Synchrotron Radiation Facility, Institute of High Energy Physics, Chinese Academy of Sciences
Beijing 100049 (P.R. China)

[+] These authors contributed equally to this work.

Supporting information for this article is given via a link at the end of the documents.

COMMUNICATION

WILEY-VCH

energy-disperse X-ray spectroscopy (EDXS) on SEM, and results show that 4.22 wt %, 4.64 wt % and negligible K^+ are in $K\text{-}\alpha\text{-MnO}_2$, $K/\alpha\text{-MnO}_2$ and $\alpha\text{-MnO}_2$, respectively (Table S1). The SEM images show that $K\text{-}\alpha\text{-MnO}_2$, $K/\alpha\text{-MnO}_2$ and $\alpha\text{-MnO}_2$ nanorods are with similar length of one to several hundreds of nanometers and diameter of twenty to thirty nanometers (Figure S1). Their specific surface areas are quite close (Figure S2 and Table S2) and their crystalline phases are all $\alpha\text{-MnO}_2$ (JCPDS No.44-0141) [7] (Figure S3), indicating that their morphology and size characteristic resembles with each other, and should not leads to significant difference in catalytic performance.

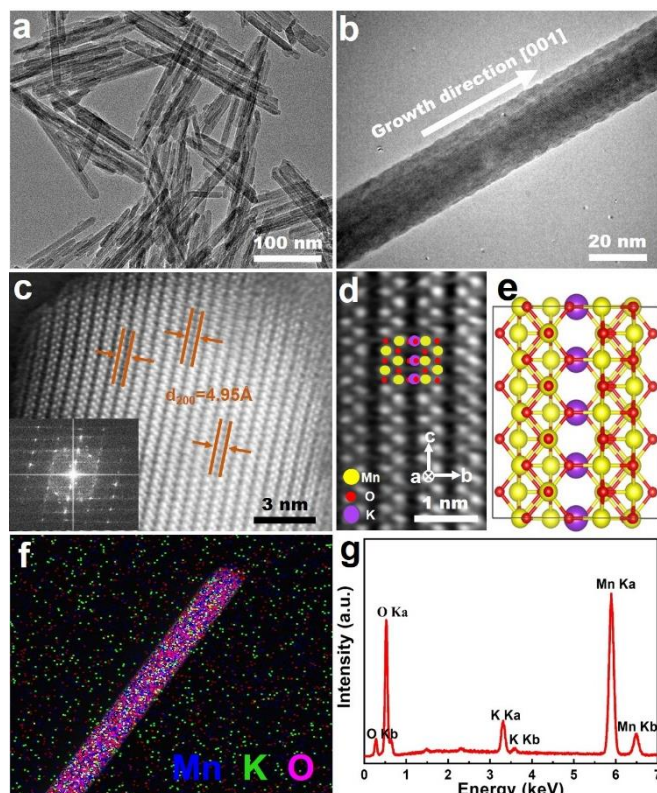


Figure 1. a) TEM image of $K\text{-}\alpha\text{-MnO}_2$ and b) one $K\text{-}\alpha\text{-MnO}_2$ nanorod along [001] direction. c) Its high-resolution HAADF-STEM image and FFT image and d) the enlarged image of c). e) Its representative atomic model. The yellow spots indicate Mn atoms, while red and purple represent O and K^+ . f) EDXS mapping of $K\text{-}\alpha\text{-MnO}_2$ nanorod. g) EDXS spectrum of the $K\text{-}\alpha\text{-MnO}_2$.

Then, their microstructure, especially for $K\text{-}\alpha\text{-MnO}_2$, were further studied using transmission electron microscopy (TEM) techniques. As shown in low-resolution TEM images (Figure 1a and 1b) and corresponding fast Fourier transform (FFT) (Figure 1c inset), the $K\text{-}\alpha\text{-MnO}_2$ is monocrystalline and grown along the [001] direction (Figure S4). [8] Then, the high-angle annular dark-field scanning transmission electron microscope (HAADF-STEM) discloses the atomic structure of $K\text{-}\alpha\text{-MnO}_2$ with exposed [200] facet, and its d_{200} spacing is 4.95 Å (Figure 1c and 1d). By observing the d_{200} spacings of $K/\alpha\text{-MnO}_2$ and $\alpha\text{-MnO}_2$ (Figure S5), it is shown that K^+ in the tunnels may slightly leads to lattice expansion. [9] Moreover, Figure 1d showed that the tunnels observed in $K\text{-}\alpha\text{-MnO}_2$ should be the 2×2 tunnels (dark stripes) surrounded by two Mn atom columns (yellow spheres). [10] The K^+ (purple spheres) were probably trapped in these 2×2 tunnels due to the proper tunnel size ($4.6 \text{ \AA} \times 4.6 \text{ \AA}$), which was depicted

based on the [100] atomic mode in Figure 1e. The EDXS of TEM (Figure 1f, 1g and S6) further confirmed that K, Mn and O were uniformly distributed over the $K\text{-}\alpha\text{-MnO}_2$, indicating the successful incorporating of K^+ .

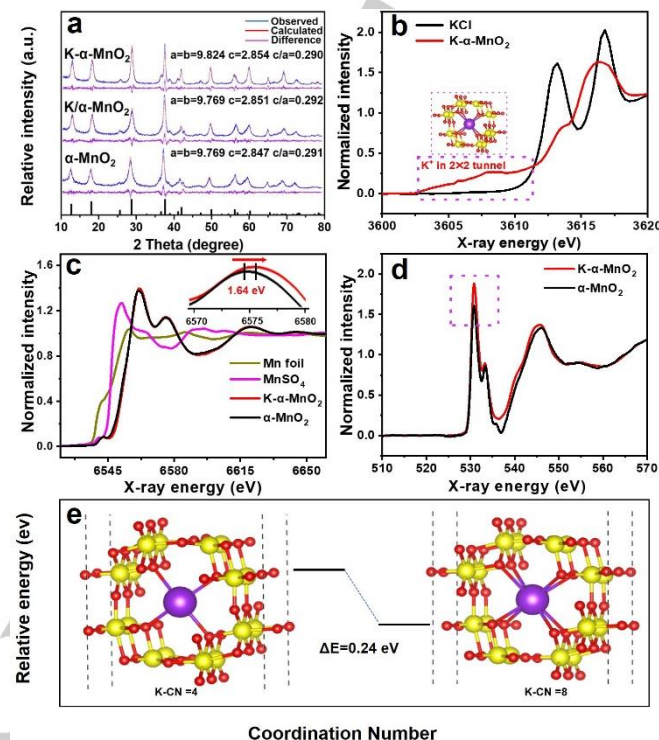


Figure 2. a) Rietveld refined XRD patterns of $K\text{-}\alpha\text{-MnO}_2$, $K/\alpha\text{-MnO}_2$ and $\alpha\text{-MnO}_2$. b) Potassium K-edge XANES spectra of $K\text{-}\alpha\text{-MnO}_2$ and KCl. c) Manganese K-edge XANES of $K\text{-}\alpha\text{-MnO}_2$ and $\alpha\text{-MnO}_2$ compared with Mn^0 (Mn foil) and Mn^{2+} ($MnSO_4$) standards. d) Oxygen K-edge XANES spectra of $K\text{-}\alpha\text{-MnO}_2$ and $\alpha\text{-MnO}_2$. e) Theoretical demonstration of K^+ position in the tunnels of $\alpha\text{-MnO}_2$ as well as site occupancy energy, CN represent the coordination numbers of K^+ with nearby O atoms.

To investigate the structural and chemical nature of K^+ in the tunnels of $K\text{-}\alpha\text{-MnO}_2$, methods including Rietveld refinement X-ray powder diffraction (XRD), the synchrotron X-ray absorption spectra (XAS) and density functional theory (DFT) were employed. Figure 2a shows the refined XRD patterns of $K\text{-}\alpha\text{-MnO}_2$, $\alpha\text{-MnO}_2$ and $K/\alpha\text{-MnO}_2$, and the a, b values (9.824 Å) of $K\text{-}\alpha\text{-MnO}_2$ are slightly larger than those of pristine $\alpha\text{-MnO}_2$ and $K/\alpha\text{-MnO}_2$ (both are 9.769 Å). This suggests that K^+ in the tunnels of $K\text{-}\alpha\text{-MnO}_2$ leads to lattice expansion along a, b axis and in line with the results of TEM observations above. Moreover, the pre-edge features of X-ray absorption near edge structure (XANES) spectra were collected for K, Mn and O elements (Figure 2b-2d). As shown in Figure 2b, the K-edge spectrum of K element for $K\text{-}\alpha\text{-MnO}_2$ shows a lower intensity pre-edge at the 3602 to 3612 eV compared with that of KCl, which further confirm that the K^+ was in the 2×2 tunnels of $K\text{-}\alpha\text{-MnO}_2$. [6b] While for O K-edge spectrum (Figure 2d), result shows that the peak intensity of $K\text{-}\alpha\text{-MnO}_2$ is higher than that of pristine $\alpha\text{-MnO}_2$, indicating the coordination environment of O atoms are correlated with the incoming K^+ . [11] Then, the features of XANES and EXAFS spectra of Mn K-edge (Figure 2c and Figure S7) were also recorded for $K\text{-}\alpha\text{-MnO}_2$ and pristine $\alpha\text{-MnO}_2$, appearing at the similar energy (6561 and 6572 eV). Compared with the Mn foil and $MnSO_4$, the Mn species of

COMMUNICATION

WILEY-VCH

the K- α -MnO₂ and α -MnO₂ are ascribed to the coexistence of Mn⁴⁺ and Mn³⁺, suggesting the insertion of K⁺ could hardly change the oxidation state of Mn in our case. This is consistent with the results of XPS measurements (details in Figure S8 and Table S3). Besides, a filter washing experiment of K⁺ was used to further confirm that the K⁺ successfully incorporated in the tunnels of K- α -MnO₂ (Figure S9 and Table S4). Furthermore, a DFT simulation is conducted (Figure 2e), and the results show that K⁺ coordinated with eight nearby O_{sp3} atoms with the coordination numbers (CN) of 8 is more energy favourable than that K⁺ coordinated with four nearby O_{sp2} atoms.

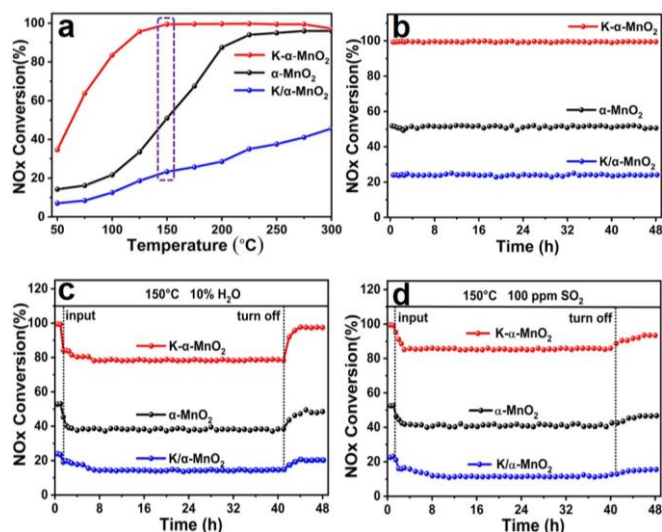


Figure 3. a) NO_x conversion ratio as a function of temperature over K- α -MnO₂, K/ α -MnO₂ and α -MnO₂. b) thermal stability test of K- α -MnO₂, K/ α -MnO₂ and α -MnO₂ at 150 °C. c) H₂O resistance. d) SO₂ tolerance. Reaction conditions: [NH₃] = [NO] = 500 ppm, [O₂] = 5 vol%, [H₂O] = 10 vol% (when used), [SO₂] = 100 ppm (when used), N₂ balance, GHSV of 60,000 h⁻¹.

Thereafter, the NH₃-SCR reactions were performed over as-prepared K- α -MnO₂, α -MnO₂ and K/ α -MnO₂ to evaluate the effect of K⁺ incorporation (Figure 3). The NO_x conversion as a function of temperature (50-300 °C) were firstly plotted (Figure 3a). Unexpectedly, compared with pristine α -MnO₂, the K- α -MnO₂ exhibited much better deNO_x performance in the low temperature of 50-200 °C. Its NO_x conversion achieved 100 % at 150 °C, which is c.a. one time higher than that of pristine α -MnO₂. Only when the temperature approaching 300 °C, the NO_x conversion of pristine α -MnO₂ can reach 100 %. While for K/ α -MnO₂, it showed poor activity in the whole temperature range due to covering of the active sites by K⁺ on the surface.^[12] Figure 3b showed the thermal stability test of the catalysts at 150 °C, and the NO_x conversion of K- α -MnO₂, α -MnO₂ and K/ α -MnO₂ maintained stable at 100 %, 50.6 % and 23.2 % during 48 h, respectively. Then, their H₂O and SO₂ tolerance (Figure 3c, 3d) were also test with additional feeding of 10 vol% H₂O vapor or 100 ppm SO₂ at 150 °C. The results show that K- α -MnO₂ exhibited an acceptable H₂O and SO₂ tolerance. Besides, the N₂ selectivity (Figure S10) and apparent activation energy based on arrhenius plots (Figure S11) of K- α -MnO₂ and pristine α -MnO₂ were also analyzed, and K- α -MnO₂ performed better for both two parameters. Moreover, the structure and morphology of K- α -MnO₂ can remain unchanged after reaction (details in Figure S12-13 and Table

S5). Generally, most NH₃-SCR catalysts showed unsatisfied performance when alkali metal species involved in the reaction.^[5] Nevertheless, in our case, the insertion of K⁺ in the tunnels greatly enhanced the low temperature activity, which inspired us to further study the atomic role of inserted K⁺ as follow.

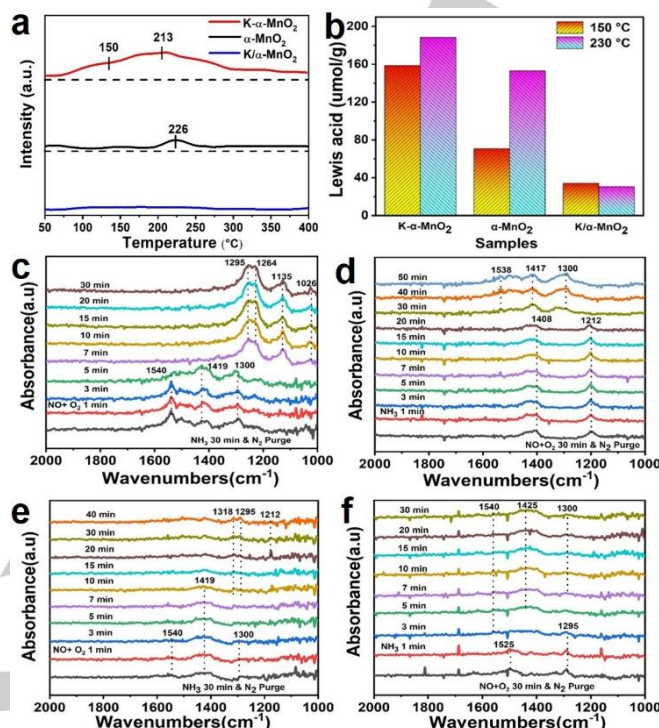


Figure 4. a) NH₃-TPD profiles and b) normalized amount of Lewis acid site of pyridine adsorption for K- α -MnO₂, α -MnO₂ and K/ α -MnO₂ at 150 °C and 230 °C. c) and d) *In situ* DRIFT spectra over K- α -MnO₂ in a flow of NO + O₂ /NH₃ after the catalyst was pre-adsorbed NH₃ / NO + O₂. e) and f) *In situ* DRIFT spectra over α -MnO₂ in a flow of NO + O₂ /NH₃ after the catalyst was pre-adsorbed NH₃ / NO + O₂.

To explore the surface chemistry and monitor the crucial intermediates, spectra mainly including the NH₃-temperature programmed desorption (NH₃-TPD), FT-IR spectra of pyridine adsorption (Py-IR) and the *in situ* DRIFT are performed and demonstrated here (Figure 4, Figure S14-S16). As shown in NH₃-TPD spectra (Figure 4a), the amount of NH₃ adsorbed on K- α -MnO₂ is much larger than those over α -MnO₂ and K/ α -MnO₂, indicating its more abundant acid sites. The peaks at 150 and 213 °C of K- α -MnO₂ were ascribed to the NH₃ chemically adsorbed on surface acid sites. The pristine α -MnO₂ showed a moderate desorption peak at 226 °C, indicating its characteristic surface acid sites. While for the K/ α -MnO₂, there was almost no desorption peak in the whole temperature range (50-400 °C). These results are consistent with their NH₃-SCR performance, indicating the surface acid sites are highly correlated with their catalytic activity. To further disclose the acidic types and amount of surface acid sites, the Py-IR was then conducted (Figure 4b, Figure S14 and Table S6). Results show that the type of surface acid sites are mainly Lewis acid sites with few Brønsted acid sites for all of the three samples (Figure S14). The amount of Lewis acid of K- α -MnO₂ (158.66 μmol/g) is one time higher than that of pristine α -MnO₂ (70.81 μmol/g) and four times higher than that of K/ α -MnO₂ (34.08 μmol/g)

COMMUNICATION

WILEY-VCH

at 150 °C. When the temperature increased to 230 °C, the amount of Lewis acid of K- α -MnO₂ (188.40 μ mol/g) is still the largest, and the amount of Lewis acid of pristine α -MnO₂ increased to 153.04 μ mol/g. However, the amount of Lewis acid of K/ α -MnO₂ kept almost unchanged. These results were in line with their catalytic performance and indicated that the incorporation of K⁺ will significantly enhanced the Lewis acid sites on the surface at low temperature, crucially for its enhanced catalytic performance.

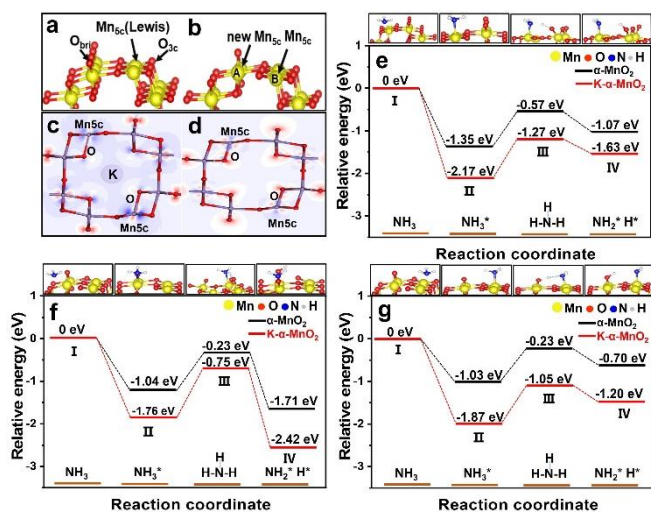


Figure 5. a) Structure of the α -MnO₂ and K- α -MnO₂ [001] surface, optimized adsorption configurations of Lewis acid Mn_{5c} site. b) Structure of the α -MnO₂ and K- α -MnO₂ [001] surface after introducing the oxygen vacancy, optimized configurations of new (A) and original (B) Mn_{5c} site. c-d) The electron density analysis of K- α -MnO₂ and α -MnO₂. e) Energy profiles of NH₃ dissociation on the Mn_{5c} site of K- α -MnO₂ and α -MnO₂ for the processes NH₃^{*} + O_{bri} → NH₂^{*} + O_{bri}H. f-g) Energy profiles of NH₃ dissociation on the new and original Mn_{5c} site of K- α -MnO₂ and α -MnO₂.

Thereafter, *in situ* DRIFT spectra of K- α -MnO₂ and pristine α -MnO₂ were performed to better understand their NH₃/NO_x adsorption/decomposition process in SCR process (Figure 4c, f and and S15, 16). For K- α -MnO₂, it was first treated with NH₃/N₂ for 30 min and then followed by purging with N₂ for 30 min at 150 °C (Figure 4c and S15a), the peaks appearing at 1419 and 1300 cm⁻¹ were attributed to coordinated NH₃ bound to Lewis acid sites,^[13] whereas no obvious bonds linked to Brønsted acid sites were observed. It is noteworthy that the amide species (-NH₂) resulting from dehydrogenation of adsorbed NH₃ was also detected (1540 cm⁻¹),^[14] which can react directly with gaseous or weakly adsorbed NO to form NH₂NO and finally decompose into N₂ and H₂O. After switching the gas atmosphere to NO + O₂, coordinated NH₃ (1419 and 1300 cm⁻¹) and the amide species (-NH₂) were decreased rapidly within 5 min. These results show that the adsorbed NH₃ species can quickly participate in the NH₃-SCR reaction. Meanwhile, some new peaks ascribed to NO_x species appeared, including the monodentate nitrate(1295, 1264 cm⁻¹),^[14a] bidentate nitrate (1026 cm⁻¹) and the disproportionation of NO bridging nitrates (1135 cm⁻¹).^[13a, 14b] In contrast, the *in situ* DRIFT spectra of reaction between pre-adsorbed NO + O₂ with NH₃ was also collected (Figure 4d and S15b). After the introduction of NH₃, both monodentate nitrate (1408 cm⁻¹) and the disproportionation of NO bridging nitrates (1212 cm⁻¹) showed rapid decrease in intensity, indicating that these

nitrate species were reactive in the SCR reaction. Meanwhile, *in situ* DRIFT spectra of pristine α -MnO₂ sample in a flow of NO + O₂ / NH₃ after pre-adsorbed NH₃ / NO + O₂ were shown in Figure 4e, 4f and S16. It is found that the ammonia species and nitrate species on the surface of α -MnO₂ were essentially the same as those on the K- α -MnO₂, implied that they have the same main reaction process. Furthermore, compared with conditions of pre-adsorption of NH₃ or NO+O₂ (Figure 4c, d and S15), results show that: 1) the pre-adsorbed peak intensity of NH₃ was much stronger than that of NO_x, 2) the NH₃ reacted with the pre-adsorbed NO+O₂ more easily than the reverse condition. It provided that NH₃ adsorption and activation should be the critical step of the NH₃-SCR in our case, which is greatly enhanced by the incorporation of K⁺ of K- α -MnO₂.

On account of NH₃ adsorption and activation is the initial and critical step of the SCR process.^[15] To uncover the atomic role of K⁺ for K- α -MnO₂, the chemical adsorption of NH₃ and dissociation of N-H bond was calculated based on DFT method (Figure 5). Experimentally, NH₃ molecules mainly adsorbed on Lewis acid sites provided by unsaturated coordinative Mn atoms with or without oxygen vacancies.^[6c] Therefore, two aspects were considered for building the models (Figure 5a, 5b, S17 and S18): 1) The adsorption of NH₃ at the original formed five-coordinated unsaturated Mn cations (Mn_{5c}, the Lewis acid site) on the (001) surface of K- α -MnO₂ and α -MnO₂, respectively (Figure 5a). 2) Oxygen vacancy is introduced by removing a two-coordinated bridge oxygen (O_{bri}) atom, then forming a new Mn_{5c} site on the surface with original Mn_{5c} site coexisted (Figure 5b).

Firstly, as shown in Figure 5e, S19 and S20, K⁺ insertion increased the adsorption energy of NH₃ on vacancy-free α -MnO₂ (-2.17 eV vs. -1.35 eV) significantly. Generally, the NH₃^{*} (* stands for the active site on the surface) was firstly activated, dissociated and then reacted with the gaseous or adsorbed NO.^[16] Whereafter, the N-H bond is broken by O_{bri} species and NH₃^{*} transformed into NH₂^{*} and H^{*} through dehydrogenation process (NH₃^{*} + O_{bri} → NH₂^{*} + O_{bri}H), the transition states were shown in Figure 5f, 5g, S19 and S20. When interfacial oxygen vacancy was formed, it is also found that no matter NH₃ adsorbed on the newly formed Mn_{5c} site or original Mn_{5c} site, the adsorption energy on K- α -MnO_{2-x} (x for the oxygen vacancy) was significantly higher than that of α -MnO_{2-x}, which is consistent with the results of NH₃-TPD. For the K- α -MnO_{2-x}, the adsorption energy of NH₃ (-1.87 eV) on the original Mn_{5c} site was higher than the new Mn_{5c} site (-1.76 eV). While the N-H dissociation energy barrier of the original Mn_{5c} site (0.82 eV) is lower than that of the new Mn_{5c} site (1.01 eV). However, the former process is an endothermic process and the later is an exothermic process. The similar phenomenon was also observed on the α -MnO_{2-x}. The adsorption energy and energy barriers of NH₃ on new Mn_{5c} site (-1.04 eV/0.80 eV) and original Mn_{5c} site (-1.03 eV/0.79 eV) are close, but the former process is endothermic (0.38 eV) and the later process is exothermic (-0.67 eV). These results revealed that incorporating K⁺ could enhance NH₃ adsorption and activation via both thermo-dynamics and kinetics way (Table S7). Moreover, the calculated Hirshfeld charge population on topmost Mn_{5c} before and after K⁺ incorporation are 0.44 and 0.47, respectively (Figure 5c and 5d), indicating that the valence electron decreases due to the charge rearrangement.^[9] This resulted in a more positively

charged Mn_{5c} site, which is more facile to adsorb and activate the NH₃ with lone pair electrons. This charge difference is consistent with the features of Mn K-edge XANES spectra (Figure 2c inset), where the Mn³⁺/Mn⁴⁺ of K- α -MnO₂ tend to move more positive valence weakly.

In summary, an unexpected phenomenon was found and demonstrated here about the alkali metal involved NH₃-SCR catalysts. As an example, after insertion of 4.22 wt% K⁺ (a common poison agent) in the tunnels, the so-called K- α -MnO₂ exhibited much better deNO_x performance than that of pristine α -MnO₂ in the temperature of 50-200 °C (100 % conversion vs. 50.6 % conversion at 150 °C). Spectroscopic and theoretical methods were then performed to study the atomic role of K⁺ in the NH₃-SCR. Results showed that K⁺ in the tunnels coordinated with eight nearby O_{sp3} atoms and then making the charge rearrangement of nearby Mn and O atoms via the columbic interactions. That resulted in more positively charged topmost five-coordinated unsaturated Mn cations (Mn_{5c}, the Lewis acid site). Therefore, these more positively charged Mn_{5c} would better adsorb and activate the NH₃ molecules, which is crucial for the subsequent reaction steps confirmed by *in situ* DRIFT spectra. This work is beneficial for further understanding the atomic role of alkali metals in Lewis acid sites dominated catalysis. Besides, it also offers a kind of potential NH₃-SCR catalyst with excellent performance at low temperature.

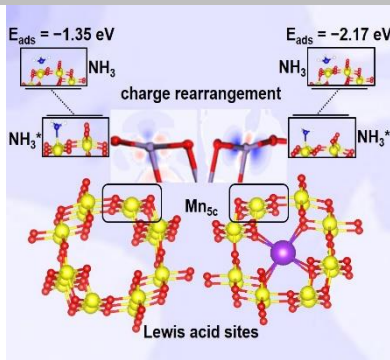
Acknowledgements

The authors gratefully acknowledged the financially support by the Natural Science Foundation of China as general projects (grant Nos. 21722702 and 21872102), and the Tianjin Commission of Science and Technology as key technologies R&D projects (grant Nos. 16YFXTSF00440, 16ZXGTSF00020, 16YFZCSF00300, 18YFZCSF00730, 18YFZCSF00770 and 18ZXSZSF00230). The authors acknowledged Prof. J. Luo for the STEM measurements.

Keywords: atomic insights • alkali metal • Lewis acid sites • NH₃-SCR • charge rearrangement

- [1] a) M. Amoyal, R. Vidruk-Nehemya, M.V. Landau, M. Herskowitz, *J. Catal.* **2017**, *348*, 29; b) M. Yang, S. Li, Y. Wang, J.A. Herron, Y. Xu, L. F. Allard, S. Lee, J. Huang, M. Mavrikakis, M. Flytzani-Stephanopoulos, *Science* **2014**, *346*, 1498; c) M. Kusche, F. Enzenberger, S. Bajus, H. Niedermeyer, A. Bosmann, A. Kaftan, M. Laurin, J. Libuda, P. Wasserscheid, *Angew. Chem. Int. Ed.* **2013**, *52*, 5028; d) A. Kaftan, M. Kusche, M. Laurin, P. Wasserscheid, J. Libuda, *Appl. Catal. B* **2017**, *201*, 169; e) X. Chen, M. Chen, G. He, F. Wang, G. Xu, Y. Li, C. Zhang, H. He, *J. Phys. Chem.* **2018**, *122*, 27331; f) J. Anton, J. Nebel, H. Song, C. Froese, P. Weide, H. Ruland, M. Muhler, S. Kaluza, *J. Catal.* **2016**, *335*, 175; g) H. Wang, W. Guo, Z. Jiang, R. Yang, Z. Jiang, Y. Pan, W.F. Shangguan, *J. Catal.* **2018**, *361*, 370.
- [2] a) Y. Ding, X. Huang, X. Yi, Y. Qiao, X. Sun, A. Zheng, D.S. Su, *Angew. Chem. Int. Ed.* **2018**, *57*, 13800; b) J. H. Docherty, J. Peng, A.P. Dominey, S. P. Thomas, *Nat. Chem.* **2017**, *9*, 595.
- [3] a) T. Kitanosono, P. Xu, S. Kobayashi, *Science* **2018**, *362*, 311; b) M. W. Schreiber, C.P. Plaisance, M. Baumgartl, K. Reuter, A. Jentys, R. Bermejo-Deval, J.A. Lercher, *J. Am. Chem. Soc.* **2018**, *140*, 4849; c) J. Chen, Y. Gao, B. Wang, T.L. Lohr, T.J. Marks, *Angew. Chem. Int. Ed.* **2017**, *56*, 15964.
- [4] a) P. Orecchia, W. Yuan, M. Oestreich, *Angew. Chem. Int. Ed.* **2019**, *58*, 1; b) M. Kim, Y. Su, A. Fukuoka, E.J.M. Hensen, K. Nakajima, *Angew. Chem. Int. Ed.* **2018**, *57*, 8235; c) W. Liu, Y. Chen, H. Qi, L. Zhang, W. Yan, X. Liu, X. Yang, S. Miao, W. Wang, C. Liu, A. Wang, J. Li, T. Zhang, *Angew. Chem. Int. Ed.* **2018**, *57*, 7071; d) J. An, Y. Wang, J. Lu, J. Zhang, Z. Zhang, S. Xu, X. Liu, T. Zhang, M. Gocyla, M. Heggen, R. E. Dunin-Borkowski, P. Fornasiero, F. Wang, *J. Am. Chem. Soc.* **2018**, *140*, 4172.
- [5] a) L. Chen, J. Li, M. Ge, *Chem. Eng. J.* **2011**, *170*, 531; b) Y. Peng, J. Li, L. Chen, J. Chen, J. Han, H. Zhang, W. Han, *Environ. Sci. Technol.* **2012**, *46*, 2864; c) S. Cimino, G. Totarella, M. Tortorelli, L. Lisi, *Chem. Eng. J.* **2017**, *330*, 92.
- [6] a) Z. Huang, X. Gu, W. Wen, P. Hu, M. Makkee, H. Lin, F. Kapteijn, X. Tang, *Angew. Chem. Int. Ed.* **2013**, *52*, 660; b) P. Hu, Z. Huang, X. Gu, F. Xu, J. Gao, Y. Wang, Y. Chen, X. Tang, *Environ. Sci. Technol.* **2015**, *49*, 7042; c) G. Zhu, J. Zhu, W. Li, W. Yao, R. Zong, Y. Zhu, Q. Zhang, *Environ. Sci. Technol.* **2018**, *52*, 8684.
- [7] S. Rong, P. Zhang, F. Liu, Y. Yang, *ACS Catal.* **2018**, *8*, 3435.
- [8] Y. Yuan, A. Nie, G. M. Odegard, R. Xu, D. Zhou, S. Santhanagopalan, K. He, H. Asayesh-Ardakani, D. D. Meng, R. F. Klie, C. Johnson, J. Lu, R. Shahbazian-Yassar, *Nano Lett.* **2015**, *15*, 2998.
- [9] L. T. Tseng, Y. Lu, H. M. Fan, Y. Wang, X. Luo, T. Liu, P. Munroe, S. Li, J. Yi, *Sci. Rep.* **2015**, *5*, 9094.
- [10] Y. Yuan, C. Zhan, K. He, H. Chen, W. Yao, S. Sharifi-Asl, B. Song, Z. Yang, A. Nie, X. Luo, H. Wang, S.M. Wood, K. Amine, M.S. Islam, J. Lu, R. Shahbazian-Yassar, *Nat. Commun.* **2016**, *7*, 13374.
- [11] D. Liu, C. Wang, Y. Yu, B.H. Zhao, W. Wang, Y. Du, B. Zhang, *Chem* **2018**, *5*, 1.
- [12] a) N. Bingwa, S. Bewana, M. J. Ndolomingo, N. Mawila, B. Mogudi, P. Ncube, E. Carleschi, B. P. Doyle, M. Haumann, R. Meijboom, *Appl. Catal. A* **2018**, *555*, 189; b) Z. Zhao, R. Yu, R. Zhao, C. Shi, H. Gies, F.-S. Xiao, D. De Vos, T. Yokoi, X. Bao, U. Kolb, M. Feyen, R. McGuire, S. Maurer, A. Moini, U. Müller, W. Zhang, *Appl. Catal. B* **2017**, *217*, 421.
- [13] a) F. Liu, W. Shan, Z. Lian, L. Xie, W. Yang, H. He, *Catal. Sci. & Technol.* **2013**, *3*; b) A. Marberger, D. Ferri, M. Elsener, O. Krocher, *Angew. Chem. Int. Ed.* **2016**, *55*, 11989.
- [14] a) J.W. Shi, Z. Fan, C. Gao, G. Gao, B. Wang, Y. Wang, C. He, C. Niu, *ChemCatChem* **2018**, *10*, 2833; b) G.Z. He, Z.H. Lian, Y.B. Yu, Y. Yang, K. Liu, X.Y. Shi, Z.D. Yan, W.P. Shan, H. He, *Sci. Adv.* **2018**, *4*, 4637.
- [15] J. Liu, Y. Wei, P.-Z. Li, P. Zhang, W. Su, Y. Sun, R. Zou, Y. Zhao, *ACS Catal.* **2018**, *8*, 3865.
- [16] H. Yuan, N. Sun, J. Chen, J. Jin, H. Wang, P. Hu, *ACS Catal.* **2018**, *8*, 9269.

The K^+ incorporated in the tunnels of α - MnO_2 , which brought a K-O eight coordination structure and the charge rearrangement of the nearby Mn and O atoms, resulted in more positively charged Mn_{5c} Lewis acid sites and an unexpectedly enhanced low temperature performance in NH_3 -SCR.



Zhifei Hao^{[a],[1]}, Zhurui Shen^{[a],[b]}, Yi Li^[c],
Haitao Wang^[a], Lirong Zheng^[d],
Ruihua Wang^[a], Guoquan Liu^[a], and
Sihui Zhan^{[a]*}

Page No. – Page No.
**Can a poison be a gift? the role of
alkali metal in the α - MnO_2 catalyzed
ammonia selective catalytic reaction**